# Energy dispersive x-ray diffraction and reverse Monte Carlo structural study of liquid gallium under pressure

O. F. Yagafarov,[1,2] Y. Katayama,[1] V. V. Brazhkin,[2] A. G. Lyapin,[2] and H. Saitoh[1]

[1]*Quantum Beam Science Directorate, Japan Atomic Energy Agency (JAEA), 1-1-1 Kouto, Sayo, Hyogo 679-5148, Japan*

[2]*Institute for High Pressure Physics, Russian Academy of Science (RAS), Troitsk, Moscow Region 142190, Russia*

(Received 23 August 2012; published 7 November 2012)

The structure of liquid gallium has been studied along the melting curve from 0.64 to 5.6 GPa by the energy dispersive x-ray diffraction technique, followed by modeling of the experimental data by the reverse Monte Carlo (RMC) method. The RMC models were constrained by the experimentally obtained equation of states of liquid Ga and in good accordance with experimental data. Analysis of the structure factor $S(Q)$ and the radial distribution function $g(r)$ shows that the anisotropic local structure of liquid Ga deviates from that of a simple hard-sphere-like liquid metal structure. Whereas the third and fourth coordination shell positions and position of the first maximum of $S(Q)$ demonstrate pressure dependencies close to a uniform compression scaled by the $(V/V_0)^{1/3}$ volume relation, the positions of the first (especially) and second coordination spheres have more flat pressure dependencies. At the same time, the first and second coordination numbers increase: The first coordination number starts from 10 to 10.5 and increases by ∼5% in the studied pressure interval. This indicates that liquid gallium contraction is nonuniform, and the local structure changes with increasing pressure. Analysis of the radial distribution function $g(r)$ by a distorted-crystalline model shows that at lower pressures liquid consists of two species similar to the solid Ga I and Ga II structures. The fraction of the Ga I-like part is about $0.2 \pm 0.05$ at 0.64 GPa, and it gradually decreases under pressure to zero at approximately $7.5 \pm 0.5$ GPa.

DOI: 10.1103/PhysRevB.86.174103 PACS number(s): 62.50.−p, 61.05.cp, 61.25.Mv

## I. INTRODUCTION

The study of the structure of gallium under extreme conditions is of fundamental interest. Due to the coaction of metallic and covalent characters of bonding,[1–4] gallium is known as a highly polymorphic metal,[5] exhibiting uncommon physical properties.[6] The stable Ga I phase is a unique example of a quasimolecular metal. At the same time, the high-pressure solid phases Ga II and Ga III have ordinary metallic properties. Solid gallium melts at moderate conditions, it has a low melting temperature (303 K) at ambient pressure, and a negative slope of its melting line (about −23 K/GPa). Liquid gallium has a structure, volume, and compressibility that are more similar to those of high-pressure phases, and is considered to be a liquid with metallic properties.[7–9] At ambient pressure the gallium melt can be easily supercooled, and the liquid-liquid transition has been reported as a possible phenomena in this state.[10,11] There have been a number of experimental and theoretical studies of liquid Ga. Experimentally, liquid gallium has been studied by a variety of techniques, such as neutron diffraction,[12–15] x-ray diffraction,[13,16–21] extended x-ray absorption fine structure (EXAFS) spectroscopy,[7,22,23] and inelastic x-ray scattering.[24,25] Most experimental studies were focused on ambient conditions, and accurate high-pressure experimental data is still of interest.

Gallium melt has a complex structure—the first peak of the structure factor $S(Q)$ has a pronounced shoulder on the high-$Q$ side that is affected by $p$-$T$ conditions.[12,17] Early studies based on pseudopotential-derived interatomic forces and an optimized random-phase approximation[26,27] show that the complex structure of liquid Ga (as well as Si and Ge) is determined by two different distance scales: the effective hard-sphere diameter expressing the geometrical requirements of sphere packing and the Friedel wavelength of the oscillatory part of the potentials, characterizing the electronic effects in the metallic bonding. A classical molecular dynamics (MD) study using a first-principles interatomic pair potential has associated anomalous features of the Ga structure factor with the occurrence of particular clusters (units with local order).[28] Namely, the most prevalent local-ordering units consist of four or five atoms, and also large clusters, corresponding to the icosahedra may be formed. A subsequent similar MD simulation[29] comprising x-ray inelastic scattering experimental data[30–33] has suggested a consistent picture. The simulation indicated that Friedel oscillations produce a modulation on the local structure of particles, which causes some stable medium-range order related to the structures beyond the first shell of the radial distribution function. According to that study, complex anomalous structures (more than 20 atoms) are involved.[29] A recent first-principles MD calculation[34] investigating the effect of high pressure on the liquid Ga structure has also supported the earlier explanation[27] that the high-$Q$ shoulder is caused by Friedel oscillations. The different explanation of the complex structure of liquid gallium employs partial-covalency effects. A first-principles MD study of the joint structural and electronic properties of liquid gallium at 1000 K revealed the formation of short-lived $Ga_2$ dimers, involving 5%–10% of all Ga atoms.[1] The high-$Q$ shoulder was attributed to these covalency remnants, with a predicted decrease of the $S(Q)$ shoulder under high-$T$ and high-$p$ conditions. Later the orbital-free first-principles simulations[35] supported the earlier proposal[1] that the shoulder was related to $Ga_2$ pairs. However, Gonzáles *et al.*[35] also showed that the concentration of pairs was larger at higher temperatures and argued the interpretation of pairs as molecular units that have survived melting.

Previous experimental studies under pressure have revealed another interesting feature of liquid gallium—the nonuniform compression. The decrease of the first nearest atomic distance

 

is smaller than is expected for a uniform compression model, therefore, changes in coordination play an important role.[7,20,36] A systematic study of the effect of pressure on the outlying coordination spheres is needed. We were motivated by the lack of detailed high-pressure experimental data that may clarify the local structural changes and contraction behavior of liquid gallium under pressure near the melting line.

Here we present an energy dispersive x-ray diffraction (EDXD) study of liquid gallium in a pressure and temperature range up to 5.6 GPa at 300–393 K, combined with reverse Monte Carlo (RMC) modeling. In comparison with previous EDXD studies,[7,17,20,21] this study provides more reliable $S(Q)$ in a larger $Q$-space interval in the specified $p$-$T$ range, resulting in a more accurate determination of the pair distribution functions. This detailed study of the radial distribution function, especially beyond the first shell, is essential for a better understanding of the structural changes of liquid gallium. Furthermore, our experimental data improves the reliability of RMC models of the gallium melt. Other advances of this work over previous RMC studies of gallium[15,21] are the wider $p$-$T$ range and reliable density constraints, based on the recent measurements of Gromnitskaya *et al.*[8] and Lyapin *et al.*[9]

## II. METHODS

*In situ* energy dispersive x-ray diffraction experiments (40–140 keV range) were carried out using a single-stage cubic-type multianvil press installed on a BL14B1 beamline at the SPring-8 synchrotron radiation facility.[37] A solid Ga sample of 99.99% purity was inserted into a pyrolytic boron nitride container inside a graphite tube heater. The assembly was placed into a pressure-transmitting medium made of a boron and epoxy resin mixture. Pressure was generated by the SMAP 180 (SPring-8 multi-anvil press, 180 ton) press machine using anvils with a $6 \times 6$ mm$^2$ square flat. The pressure was determined by NaCl markers[38] placed under the sample container. Heating was produced by passing the alternating current through a graphite heater, and the temperature was measured directly by a chromel-alumel thermocouple. The estimated absolute errors were within ~0.2 GPa and ~3 K for experiments at 300 K and ~10 K for experiments at higher temperatures.

Diffraction patterns were collected with a solid-state detector at several diffraction angles in the range 4°–21° (with 2°–3° steps) for up to 4000 s at the highest angle. The structure factor $S(Q)$ was determined using the previously developed method.[39,40] In order to reduce the effect of potential errors in $S(Q)$, such as termination error and errors in normalization and scattering factors, we have used the procedure described by Kaplow *et al.*[41] The radial distribution function $g(r)$ was obtained by a Fourier transformation of $S(Q)$ with a modified Welch window function.[42]

The density approximation for liquid is based on previous ultrasonic measurements of the bulk modulus of gallium.[8,9] To calculate the equation of state for liquid gallium we have used the following values of the isothermal bulk modulus and its pressure derivative near room temperature, $B_0 = 50 \pm 3$ GPa and $B_0' = 1$, where the correction of the volume related to the change of temperature along the melting curve was negligible.[9]

This approximation is in good agreement with the existing, much earlier data for compressibility of gallium at low pressures.[43] The values of the isothermal bulk modulus and its pressure derivative determined from the polynomial approximation given by Köster *et al.* are $B_0 \sim 45.3$ GPa and $B_0' \sim 1$.[43] A recent paper[25] on an inelastic x-ray scattering study of liquid gallium gives estimates of density values close to our calculations: 6.33 and 6.73 g/cm$^3$ at 0.8 GPa, 295 K, and at 6.1 GPa, 393 K, respectively. The comparison between the different data is presented in Fig. 1. Another high-pressure approximation is based on density variation; this yields the best fit of the experimental $S(Q)$ data in RMC simulations.[21] The weak point of such an approach is that RMC modeling lacks constraints, since this method typically has more variables than observables. Therefore, without the appropriate use of explicit constraints, the reliability of the final configuration becomes fairly low. As a result, such an approach overestimates the density values under pressure, corresponding to an unlikely low bulk modulus [$B_0 = 12.1(6)$ GPa and $B_0' = 4$].[21]

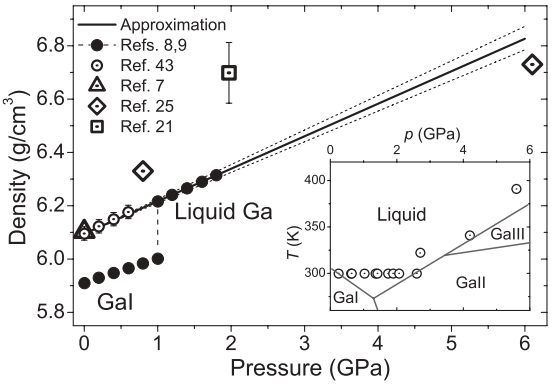


FIG. 1. The density approximation for liquid gallium under pressure compared with previous results. The data from the ultrasonic measurements at 285 K (black circles) show the melting of solid Ga I at 1 GPa under compression. The inset shows the selected experimental points on a phase diagram.

The reverse Monte Carlo technique was applied to the experimental $S(Q)$ data. All the models consist of 10 000 Ga atoms in cubic boxes with periodic boundary conditions. First, a random initial configuration with a density constraint is modified to satisfy the condition that no two atomic centers are within 2.2 Å of each other (cutoff distance constraint). The result is a starting configuration represented by the maximally disordered system that satisfies the explicit constraints. Experimental $S(Q)$ data have been modeled then using RMC++ software.[44] The resulting atomic configurations represent the possible models of the studied structure.

## III. RESULTS AND DISCUSSION

A solid gallium sample melts easily under loading.[45,46] A number of *in situ* x-ray diffraction measurements have been performed during isothermal compression of liquid gallium at room temperature, before the sample solidified. Several measurements have been made under pressure above the melting line, after heating the sample at constant load. The melting is judged from the significant increase of the halo pattern in the absence of crystalline diffraction peaks.

Figure 2(a) shows the structure factor $S(Q)$ obtained for liquid gallium at selected $p$-$T$ conditions. The structure factor

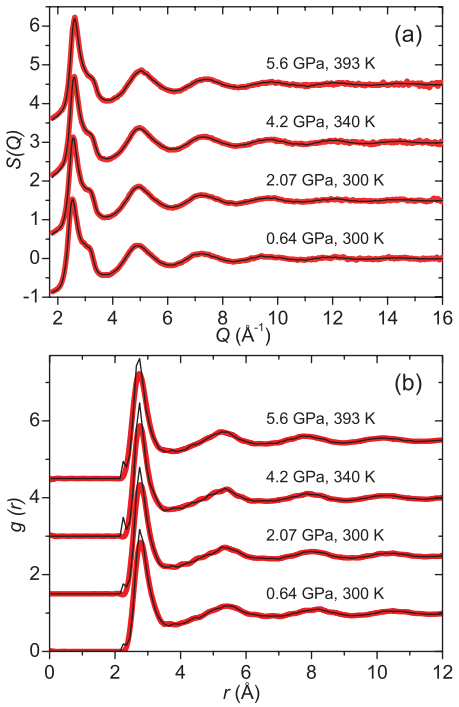


FIG. 2. (Color online) (a) Structure factors $S(Q)$ and (b) radial distribution functions $g(r)$ of liquid gallium from experiments (thick red lines) and from RMC models (thin black lines) at selected $p$-$T$ conditions.

at the lower energy region cannot be obtained using the present technique due to background scattering and absorption in a large-volume press. The shape of the measured structure factor at the lowest pressure is in agreement with previous data obtained by the neutron and x-ray diffraction experiments at ambient conditions.[12,13] The quality of the RMC fit to the experimental $S(Q)$ data is also presented in Fig. 2. Good agreement between the experimental $S(Q)$ and the model supports our estimates of the density of liquid gallium under pressure. The radial distribution functions derived from the RMC models are also very close to the experimental ones [Fig. 2(b)]. However, the calculated $g(r)$ has a small spike just after the cutoff distance (2.2 Å). It was also observed in the previous RMC analysis of neutron diffraction data on the gallium melt at normal pressure.[15] Similar to previous authors, we have found that suppressing this spike induced a configuration change with a negligible effect on the statistical analysis.

It is known that for most simple, hard-sphere-like liquid metals, the first peak of the structure factor is quite symmetrical; the ratios of the positions of the second peak to the first peak of both $S(Q)$ and $g(r)$ have typical values close to $Q_2/Q_1 \approx 1.86$ and $r_2/r_1 \approx 1.91$.[26,47] However, for liquid gallium the first peak of $S(Q)$ has a well-pronounced high-$Q$ shoulder and an abnormally high value of the ratio $Q_2/Q_1 \approx 1.94$ at 0.64 GPa. Similar deviations from typical values have been reported earlier, for example, for liquid Ga, Si, Bi, and others.[16,26,47] Such a high $Q_2/Q_1$ value manifests some of the complexity of the liquid gallium structure. With increasing pressure, the peak positions shift slightly to higher-$Q$ values. The height of the first peak increases, while the

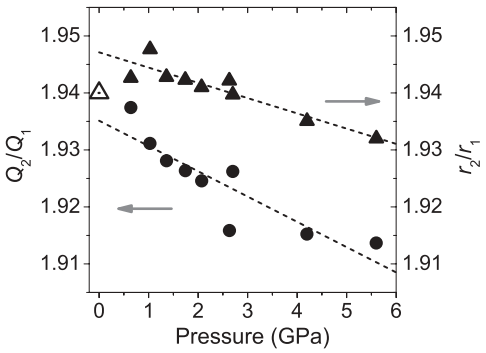


FIG. 3. Pressure dependencies of ratios of the position of the second peak to that of the first peak in the structure factor (circles) and radial distribution function (our data: solid triangles; data from Ref. 16: open triangles).

height of the shoulder slightly decreases under pressure. The first peak in the experimental radial distribution function is also rather asymmetric and has a small shoulder on the high-$r$ side. This shoulder remained for the whole range of experimental $p$-$T$ conditions. The values of both $Q_2/Q_1$ and $r_2/r_1$ ratios (see Fig. 3) tend to decrease with increasing pressure and temperature, suggesting a gradual change of gallium melt to the hard-sphere-like structure. However, even at the highest pressure, the ratios are still larger than those for simple liquids, which implies the persistence of some local anisotropy. A simple linear approximation gives the pressure ~15 GPa where the ratio values should become similar to those for simple hard-sphere-like liquid metals.

The positions of the first four peaks in $g(r)$ at the lowest pressure are 2.788(3), 5.42(1), 8.13(2), and 10.52(3) Å. The shift of the first peak position and the following minimum in the radial distribution function of liquid gallium are found to be smaller than 0.05 Å for compression from 0.64 up to 5.6 GPa. The height of the first peak depends slightly on $p$-$T$ conditions: It increases under pressure and decreases at higher temperatures. A similar behavior of the first peak was also reported in previous studies.[7,20,21] More detailed experimental data allow analyzing the positions accurately.

An interesting result has emerged from the study of the effect of pressure on the first four coordination spheres. Figure 4 represents the first four neighbor distances as functions of density. The position $r_i$ of the $i$th peak in the pair distribution function $g(r)$ is normalized to that at ambient conditions $r_i(0)$. It is well known that for uniformly compressed liquid metals all $r_i/r_i(0)$ ratios follow the $(V/V_0)^{1/3}$ relation [e.g., liquid alkali metals K and Na (Refs. 48 and 49)]. In the case of gallium these dependencies clearly indicate completely different behavior. The decrease of the nearest atomic distances $r_1$ and $r_2$ is considerably smaller than that expected for the uniform compression model, whereas $r_3/r_3(0)$ and especially $r_4/r_4(0)$ values are much closer to the $(V/V_0)^{1/3}$ relation (Fig. 4). The moderate decrease in $r_1/r_1(0)$ and $r_2/r_2(0)$ values indicates that the densification of gallium may be due to short-range order, namely, the increase in the first and second coordination numbers ($N$s). At the same time, the farther coordination spheres (third and fourth) are characterized by atomic density averaged over larger numbers of atoms and by distances with a considerably lower effect of

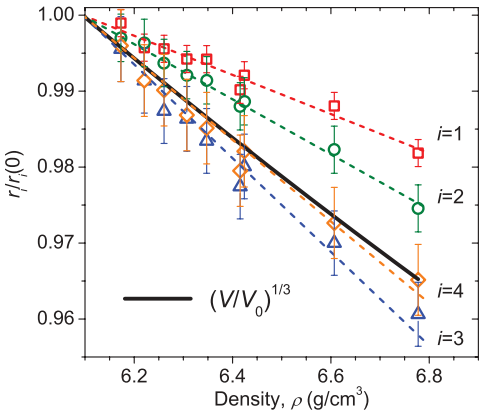


FIG. 4. (Color online) The comparison of density dependence of the first four neighbor distances $r_i/r_i(0)$ with the relation $(V/V_0)^{1/3}$.

structural correlations, therefore, they agree better with bulk densification of gallium.

The first coordination number behavior under pressure is presented in Fig. 5. Indeed, densification results mostly in the increase of the first coordination number. The values have been obtained from both experimental data and RMC configurations. To calculate $N$ from a radial distribution function $T(r) = 4\pi r^2 \rho_0 g(r)$, we have used two common methods[12,47] to define the area under the first peak (see the inset to Fig. 5). The first approach considers the right- and left-hand sides of the first peak to be symmetrical. Therefore, the area is determined as the integral of $T(r)$ from $r_0$ to $r_{max}$ multiplied by 2. The calculated $N_{sym}$ may be considered to be the lower limit, since the first peak is not truly symmetrical. Thus, another method to obtain the coordination number is to

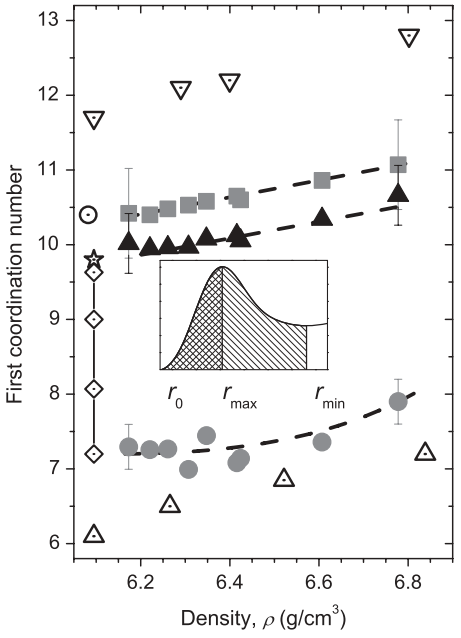


FIG. 5. The first coordination number calculated by different methods. Our data $N_{min}$ (solid triangles), $N_{RMC}$ (solid squares), $N_{sym}$ (solid circles) is compared with previous results from Ref. 12 as open diamonds, Ref. 17 as open triangles, Ref. 16 as open circles, Ref. 23 as open stars, and Ref. 34 as open reverse triangles.

calculate the area of the first peak by integrating $T(r)$ in from the left-hand edge $r_0$ to the first minimum $r_{min}$ on the right-hand side. The edge $r_0$ can easily be defined. However, even after reducing ripples in the radial distribution function, the $r_{min}$ value is not rigid and can fluctuate due to the contribution of different errors. The final integral value of $T(r)$ is sensitive to such fluctuations, therefore, considering minor changes in the first peak position, the value of $r_{min}$ is averaged for all curves at different $p$-$T$ points. The $N_{min}$ value calculated in this way is considered to be the upper limit of the number of atoms. In a similar way, the average $N_{RMC}$ value is obtained from RMC configurations. The number of neighbors within predefined distances ($r_0 = 2.35$ Å and $r_{min} = 3.55$ Å) can be calculated directly in the atomic configuration. The contribution of the spike before the first peak in calculated $g(r)$ (see Fig. 2) is small (<1%), but nevertheless has been avoided.

It is known that the coordination number value for most of liquid metals that have a normal close-packed structure is about 11–12. For example, the coordination number for liquid Al is 11.5 (compared with 12 for crystal phase).[47] Metals with a relatively open packed structure usually have lower coordination. The coordination number for the unique solid Ga I phase is 7, and for the liquid phase it is about 10 (Fig. 5). The calculated $N$ values and their increase under pressure correlate well with previous results of experimental and theoretical work. It should be noted that the absolute values of $N$ strongly depend on the definition used[12] (see the typical range in Fig. 5). However, $N_{min}$ values should be closer to real $N$, as the asymmetry of the coordination shell has to be considered. Furthermore, taking into account the high quality of the experimental data and the consistent RMC modeling (with reasonable density constraints), the most reliable values for the first $N$ should be close to 10–10.5 at the lowest pressure and 10.5–11 at the highest pressure in our experiments. A gradual increase of the $N$ is also associated with a decrease in the anomaly of the liquid gallium structure. Additional evidence for this conclusion can be provided by the comparison of $N_{sym}$ and $N_{min}$ values. Their difference corresponds directly to the degree of distortion of the atomic arrangement relative to a simple hard-sphere-like structure. For example, for noble-gas liquids $N_{sym} \sim 8$–9 and $N_{min} \sim$ 10–11;[50] for liquid Cu, $N_{sym} = 10.3$ and $N_{min} = 11.3$.[47] In the case of gallium, the relative difference of the $N_{sym}$ and $N_{min}$ values is bigger and tends to decrease at higher pressures due to a slightly larger increase of the $N_{sym}$.

The behavior of the averaged $N_{RMC}$ dependence is consistent with that directly derived from the radial distribution function. Figure 6(a) represents the distribution of coordination numbers of the atoms in RMC configurations within 2.35–3.55 Å. It can be noted that while the nearest-neighbor distance does not change much with densification, the number of atoms with larger $N$ grows, increasing the mean $N_{RMC}$ value from 10.4 at the lowest pressure to 11.1 at the highest. The width of the distribution remains the same, and gallium atoms in RMC configurations have from seven to 14 neighbors.

The partial radial distribution functions $G_i(r)$, $i = 1, \ldots, 12$ at the lowest and highest pressures are shown in Fig. 6(b). The definition of $G_i(r)$ denotes the probability of finding the $i$th neighbor of a random atom at a distance $r$.[51] The variation of $G_i(r)$ with densification can be analyzed.

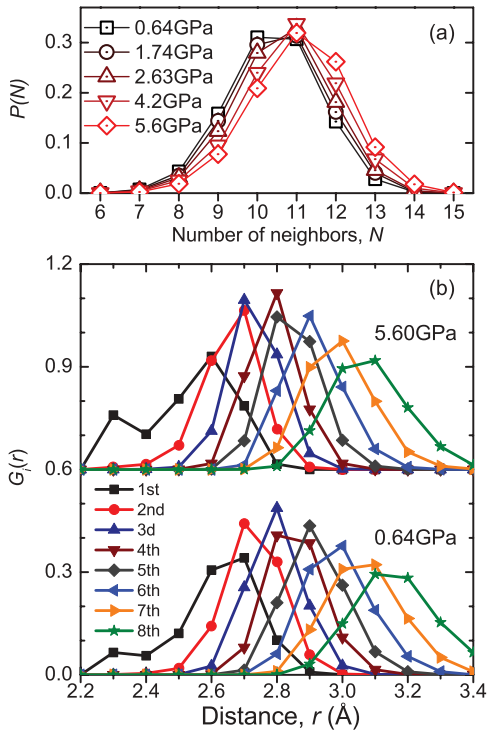


FIG. 6. (Color online) Structural details of RMC models at selected experimental $p$-$T$ points: (a) $N$ distributions for neighbors within 2.35–3.55 Å from the lowest (0.64 GPa at 300 K, black squares) to the highest (5.6 GPa at 393 K, bright red diamonds); (b) partial radial distribution functions $G_i(r)$, where $i$ is the index of the neighbor at 0.64 GPa at 300 K and 5.6 GPa at 393 K (shifted along the $y$ axis for clarity).

Densification under compression does not change much the height and width of the corresponding peaks, and slightly affects the displacement of peak positions (less than 2.5% in the experimental pressure range). Analysis of the $G_i(r)$ distributions can shed some light on the question of the presence of $Ga_2$ dimers in liquid gallium. The presence of dimers should result in a well-defined separation of the first sharp peak from the $G_1(r)$ distribution due to a typical covalent bonding distance of 2.25–2.5 Å.[1] With increasing pressure and temperature, the number of dimers should decrease. According to our study, at lowest pressures there is no such splitting of the $G_1(r)$ distribution. As was pointed out before, the small peak at 2.3 Å is caused by RMC modeling and most likely cannot be associated with $Ga_2$ dimers. It appears just after the cutoff distance used for modeling, and in the case of RMC modeling without the cutoff distance, its position shifts to smaller distances. Another possible argument is that this peak does not decrease at higher pressures, as a dimer-caused peak should. Thus, there is no clear evidence of the presence of $Ga_2$ dimers in the RMC configurations obtained from our experimental data, and most probably a number of dimers in the models is very small.

In Fig. 7 we demonstrate the triplet correlations, i.e., the angle distribution between three atoms in a configuration within a cutoff distance of 3.55 Å. The gallium bond angle distribution function featuring two peaks is similar to that for simple elemental liquids. At the lowest

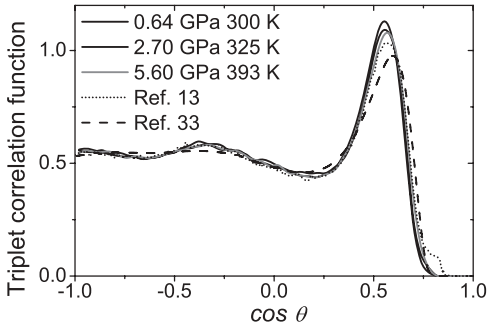


FIG. 7. The triplet correlation function for liquid gallium calculated from the RMC models at selected $p$-$T$ conditions, compared with data from Refs. 15 and 35.

pressure, the two maxima are close to icosahedral angles: the broader one at $\sim\arccos(-0.35) \approx 111^\circ$ and the narrow one at $\sim\arccos(0.55) \approx 57^\circ$. The formation of icosahedralike clusters (consisting of small clusters) has been found in MD models of gallium at 473 K.[28] However, the icosahedral coordination number is 12, and as one can see from Fig. 6, this number of neighbors is not exceptionally preferable for RMC models. Thus here we should stress that we are dealing with an average bond orientational order within the first coordination shell only, and this should not be interpreted as the existence of well-defined icosahedralike clusters in liquid gallium. Rather we can consider these data comparatively: Compression results in a slight shift of the narrow peak to $\sim 55^\circ$. In the case of simple liquids, triplet correlations usually have a main peak at 54.5°–49.5°,[52] so this trend is also consistent with the idea of changing the liquid gallium structure to be closer to a simple liquidlike structure.

Another interesting point is the dependence of the first peak position $Q_1$ of $S(Q)$ versus density or atomic volume [$v_a = M/(N_A\rho)$, where $N_A$ is Avogadro's number and $M$ is the atomic weight]. Note that, as $v_a$ decreases under pressure from 18.76 to 17.08 Å$^3$ (by ~9%), $Q_1$ increases from 2.53 to 2.62 (by ~3.5%). Plotting $Q_1$ vs $v_a$ on a logarithmic scale revealed a scaling relationship, as shown in Fig. 8. From a fundamental point of view, such a dependence is used to discuss structural changes under pressure. From a practical point of view it is essential for experiments with a limited measurable $Q$ range (e.g., in diamond anvil cells). In the case of simple elastic compression the change in $Q_1$ is related

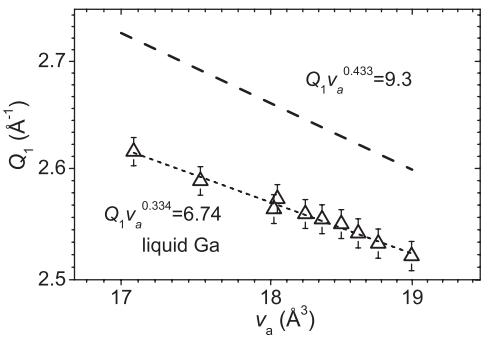


FIG. 8. Power-law scaling of the first peak $Q_1$ vs atomic volume $v_a$. Both $Q_1$ and $v_a$ are on a logarithmic scale. The straight dashed lines are given as guides to the eye.

to the decrease in the volume, $(V/V_0)^{1/3} = d/d_0 \sim Q_{10}/Q_1$, where $d \sim 2\pi/Q_1$ and the subscript 0 refers to values at ambient pressure. For example, for metallic glasses usually such uniform compression is assumed, $Q_1 \sim v_a^{-1/3}$ corresponding to a dense random packed structure.[53,54] However, another power-law scaling was recently reported for several different metallic glasses at ambient pressure. The proposed scheme of self-similar packing of atomic clusters yields the relation $Q_1 v_a^{0.433\pm0.007} = 9.3 \pm 0.2$.[55] Similarly, a previous high-pressure study of the silica glass showed that the shift of the first diffraction peak with pressure is inconsistent with the simple elastic compression of $SiO_2$ glass due to structural changes in the medium-range order described by the first diffraction peak in $S(Q)$.[56]

For liquid gallium under compression, our experimental data give the relation $Q_1 v_a^{0.334\pm0.01} = 6.74 \pm 0.3$. The proximity of the power value obtained to the typical value of $1/3$ correlates with our conclusion made earlier, that the bulk densification of gallium agrees better with the averaged compaction of the further coordination spheres that have a larger contribution to the first peak $Q_1$ in the structure factor. In this sense, a sensible result is obtained for the equation involving the second peak position, $Q_2 v_a^{0.242\pm0.02} = 9.97 \pm 0.64$. As it was stated earlier, the value of the $Q_2/Q_1$ ratio for gallium is higher than for simple liquids, and tends to decrease. This results in a considerable deviation of the power value from $1/3$ and a large constant on the right-hand side.

Finally, in order to examine local structural changes in liquid gallium, we have compared the contraction behavior of liquid gallium and several crystalline phases. We used a distorted-crystalline model to simulate $g(r)$ for liquid from crystalline data by giving a Gaussian-type distribution for the interatomic distances.[57] One should note that this method does not provide a universal way to represent exactly the liquid structure. However, it allows to conveniently describe the features and trends in the local structural changes. We started by examining the similarity of the liquid gallium structure to the solid gallium structures, as well as to the typical fcc and bcc structures. At ambient conditions, the Ga I phase has a base-centered orthorhombic structure, formed by eight gallium atoms.[58] In high-pressure phases, Ga II has a complex 104-atom C-face-centered orthorhombic structure[5] that can be represented as a distorted body-centered structure, while Ga III has a more simple, body-centered tetragonal structure,[45] stable up to 120 GPa, where it transforms to a Ga IV phase with a fcc structure.[59] Experimentally determined $g(r)$ for liquid gallium has been compared with simulated crystal structures of the same number density. The lattice parameters for each simulated structure were estimated from the number density of gallium melt at every $p$-$T$ experimental point. We used previously reported structural parameters for these estimates.[5,45,58]

The simulated $g(r)$ for high-pressure phases, especially Ga II, shares the general features of the experimental $g(r)$ for liquid gallium closer than does $g(r)$ for Ga I (Fig. 9). The $g(r)$ simulated for other crystal structures such as bcc, fcc, or hcp could not accurately reproduce the experimental $g(r)$. It is interesting to compare the ratios of the positions of the second and first peaks of the simulated $g(r)$ for solid Ga I, Ga II, Ga III, bcc, and fcc structures: 1.59, 1.91, 1.74, 1.82, and 1.75 correspondingly. The ratios for Ga II and bcc are most similar to those of the simple hard-sphere-like liquid metals. Even for Ga II there is still some discrepancy observed between the experimental and simulated $g(r)$, most notably around the second peak and the preceding minimum. Therefore, we can assume that the liquid structure cannot be described by one local structure and may consist of a mixture of two local structures, similar to those observed in crystalline phases.

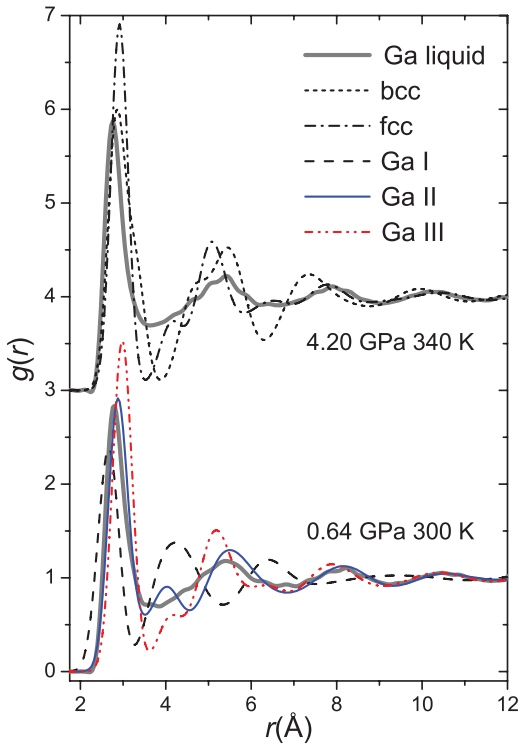


FIG. 9. (Color online) Comparison of $g(r)$ measured for the gallium melt (thick gray lines) at 0.64 GPa at 300 K and at 4.2 GPa at 340 K, with those simulated for several solid structures with the same number density.

In order to verify this idea, the total simulated $g_{\text{calc}}(r)$ for liquid gallium was expressed by a simple linear combination of $g_n(r)$ for the two components: $g_{\text{calc}}(r) = (1 - x)g_1(r) + xg_2(r)$. The fitting of the observed $g(r)$ with the $g_{\text{calc}}(r)$ has been made by varying the contribution of the second component $x$, while fixing the other parameters. The gradual decrease in the short-range order with the increase of the interatomic distance was simulated by the increasing dispersion of the Gaussian $\sigma_i = (r_i/r_1)\sigma_1$,[57] where $\sigma_1 = 0.2$. Several combinations of crystalline structures have been tested. To compare them, the goodness-of-fit parameter $R = \sqrt{\frac{1}{N}\sum_{i=0}^{N-1}[g_{\text{expt}}(r_i) - g_{\text{calc}}(r_i)]^2}$ has been used. Selected results of simulations at different $p$-$T$ conditions are presented in Fig. 10. The $g(r)$ simulated for a system of two local structures, better than the single-structure models, fits the $g(r)$ for liquid gallium [Fig. 10(a)]. However, some, albeit smaller, discrepancy just before the second peak is still observed.

To formalize the selection of the appropriate components and their ratios, we compared the $R(x)$ parameter

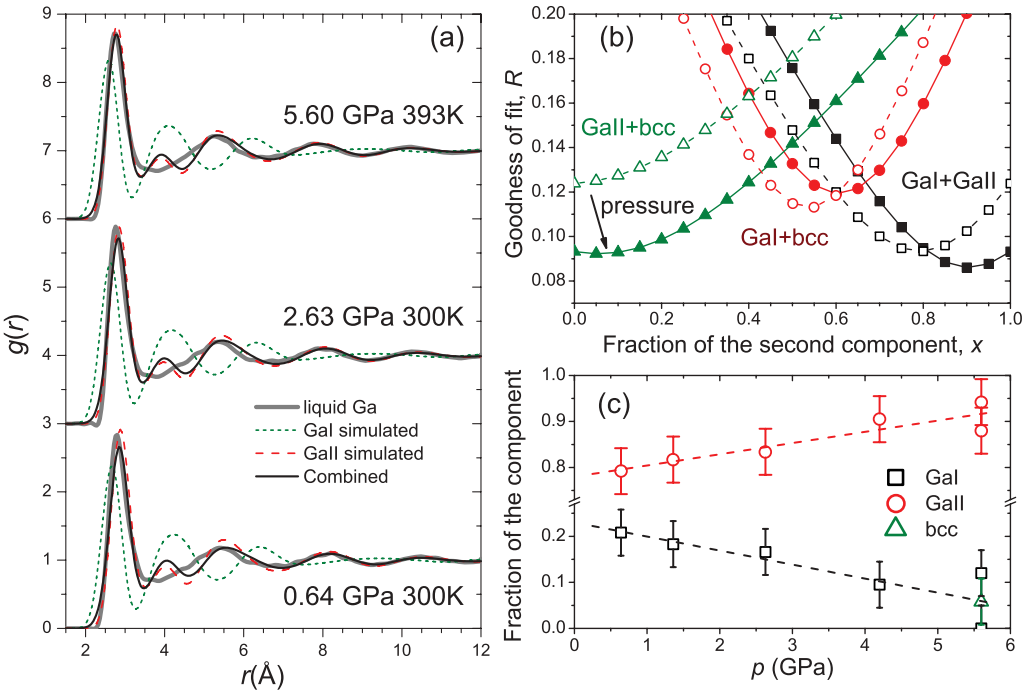


FIG. 10. (Color online) (a) Experimental and simulated $g(r)$ for liquid Ga; (b) comparison of the goodness of fit parameter $R$ for different combinations of local structures used in simulations. Curves for low pressure (0.64 GPa, 300 K, open symbols) and high pressure (4.20 GPa, 340 K, solid symbols) are given. (c) Pressure-induced change of component fractions for the best fit combinations.

dependencies at different experimental conditions. At the lowest pressure, the best fit was obtained by using the combination of Ga I and Ga II local structures [Fig. 10(b)]. Other combinations that have comparatively small values of the minimal $R$ parameter are also shown in the figure. Increasing pressure affects the ratios: At 4.2 GPa the combination of Ga I with a bcc structure becomes even less favorable, whereas $g(r)$ calculated for Ga II with a small amount of bcc structure improves considerably. However, in this case the minimal $R$ parameter value is slightly larger than that for $g(r)$ calculated for Ga I with Ga II. Thus, the fractions of the Ga I-like and Ga II-like local structures are given in Fig. 10(c). The behavior of the fractions demonstrates that the local structure of liquid gallium gradually changes to be more Ga II-like. This view is consistent with the observed increase of the first coordination number in liquid gallium, as each atom is surrounded by seven others in Ga I and by ten others in Ga II structures.

If we assume that the change in the local structure of liquid gallium is continuous, then the linear approximation gives the pressure value of ∼7.5 GPa; beyond that the Ga I-like structure contribution should vanish completely. Uncertainty in the fraction value $\Delta x \approx \pm 0.05$ has been estimated from the residuals of the fitting; for the highest pressure of 5.6 GPa it makes the models Ga I with a Ga II structure and Ga II with a bcc structure almost equal. Assuming that further compression makes the structure of liquid gallium more as a simple liquid, we suggest that the fraction of the bcc local structure will increase, as $g(r)$ simulated for the bcc-like local structure with the distortion usually fits well the $g(r)$ of simple liquids.[57] Continuous structural changes in liquid Ga observed in the present work do not contradict a possible more sharp liquid-liquid transition in the deeply undercooled state.[10,11]

## IV. CONCLUSIONS

In this work we have studied liquid gallium structure changes under pressure, along the melting line up to 5.6 GPa using the EDXD experimental technique and RMC modeling. The RMC models accurately reproduce structure factors measured at different $p$-$T$ conditions, as an employment of the experimental density constraints makes the structural RMC analysis more reliable. The results of the study are summarized as follows.

(i) An anisotropic contraction of the local structure occurs continuously in liquid gallium, expressed as a moderate decrease of the nearest coordination spheres. Study of a high quality structural experimental data, together with consistent RMC model, shows a moderate increase of the first coordination number in comparison with the data obtained previously and based on a rough approximation of density. Our experimental data suggest a gradual change of gallium melt to a simple hard-sphere-like liquid metal at ∼15 GPa.

(ii) The local structure of liquid gallium can be described as similar to the mixture of two local structures, Ga I-like and Ga II-like. The fraction of the low-pressure Ga I-like structure decreases continuously under pressure, reaching zero at about 7.5 GPa.

(iii) Analysis of the RMC modeled atomic configurations has not revealed the existence of $Ga_2$ dimers. The analysis supports the view that the liquid gallium structure approaches a simple-liquid-like structure.

## ACKNOWLEDGMENTS

We gratefully acknowledge E. Gromnitskaya, T. Watanuki, L. Temleitner, S. Kohara, K. Tsuji, and T. Hattori for their

valuable discussions. This work was supported in part by the Grant-in-Aid for Scientific Research on Innovative Areas (Grant No. 20103004) from the Ministry of Education, Culture, Sports, Science and Technology of Japan, by the Russian Foundation for Basic Research (Grants No. 10-02-01407 and No. 11-02-00303), and by the Programs of the Presidium of the Russian Academy of Sciences. The experiments on BL14B1 were performed with the approval of the Japan Synchrotron Radiation Research Institute (Proposals No. 2010B3604 and No. 2011A3606).

[1]X. G. Gong, G. L. Chiarotti, M. Parrinello, and E. Tosatti, Phys. Rev. B **43**, 14277 (1991).
[2]U. Häussermann, S. Lidin, S. I. Simak, and I. A. Abrikosov, Chem. Eur. J. **3**, 904 (1997).
[3]D. A. Walko, I. K. Robinson, C. Grütter, and J. H. Bilgram, Phys. Rev. Lett. **81**, 626 (1998).
[4]M. Bernasconi, G. L. Chiarotti, and E. Tosatti, Phys. Rev. B **52**, 9988 (1995).
[5]O. Degtyareva, M. I. McMahon, D. R. Allan, and R. J. Nelmes, Phys. Rev. Lett. **93**, 205502 (2004).
[6]R. W. Powell, M. J. Woodman, and R. P. Tye, Br. J. Appl. Phys. **14**, 432 (1963).
[7]L. Comez, A. Di Cicco, J. P. Itié, and A. Polian, Phys. Rev. B **65**, 014114 (2001).
[8]E. L. Gromnitskaya, O. F. Yagafarov, O. V. Stalgorova, V. V. Brazhkin, and A. G. Lyapin, Phys. Rev. Lett. **98**, 165503 (2007).
[9]A. Lyapin, E. Gromnitskaya, O. Yagafarov, O. Stalgorova, and V. Brazhkin, J. Exp. Theor. Phys. **107**, 818 (2008).
[10]C. Tien, E. V. Charnaya, W. Wang, Y. A. Kumzerov, and D. Michel, Phys. Rev. B **74**, 024116 (2006).
[11]S. Cajahuaringa, M. de Koning, and A. Antonelli, J. Chem. Phys. **136**, 064513 (2012).
[12]P. Ascarelli, Phys. Rev. **143**, 36 (1966).
[13]A. H. Narten, J. Chem. Phys. **56**, 1185 (1972).
[14]M. C. Bellissent-Funel, P. Chieux, D. Levesque, and J. J. Weis, Phys. Rev. A **39**, 6310 (1989).
[15]V. M. Nield, R. L. McGreevy, and M. G. Tucker, J. Phys. Condens. Matter **10**, 3293 (1998).
[16]Y. Waseda and K. Suzuki, Phys. Status Solidi B **49**, 339 (1972).
[17]K. Tsuji, J. Non-Cryst. Solids **117–118**, 27 (1990).
[18]K. Yaoita, M. Imai, K. Tsuji, T. Kikegawa, and O. Shimomura, High Press. Res. **7**, 229 (1991).
[19]K. Tamura and S. Hosokawa, J. Non-Cryst. Solids **156–158**, 650 (1993).
[20]L. Ehm, S. M. Antao, J. Chen, D. R. Locke, F. Marc Michel, C. David Martin, T. Yu, J. B. Parise, S. M. Antao, P. L. Lee, P. J. Chupas, S. D. Shastri, and Q. Guo, Powder Diffr. **22**, 108 (2007).
[21]T. Yu, J. Chen, L. Ehm, S. Huang, Q. Guo, S.-N. Luo, and J. Parise, J. Appl. Phys. **111**, 112629 (2012).
[22]R. Poloni, S. De Panfilis, A. Di Cicco, G. Pratesi, E. Principi, A. Trapananti, and A. Filipponi, Phys. Rev. B **71**, 184111 (2005).
[23]S. Wei, H. Oyanagi, W. Liu, T. Hu, S. Yin, and G. Bian, J. Non-Cryst. Solids **275**, 160 (2000).
[24]S. Hosokawa, M. Inui, Y. Kajihara, K. Matsuda, T. Ichitsubo, W.-C. Pilgrim, H. Sinn, L. E. González, D. J. González, S. Tsutsui, and A. Q. R. Baron, Phys. Rev. Lett. **102**, 105502 (2009).
[25]V. M. Giordano and G. Monaco, Phys. Rev. B **84**, 052201 (2011).
[26]J. Hafner and G. Kahl, J. Phys. F **14**, 2259 (1984).
[27]J. Hafner and W. Jank, Phys. Rev. B **42**, 11530 (1990).
[28]S.-F. Tsay and S. Wang, Phys. Rev. B **50**, 108 (1994).
[29]K. H. Tsai, T.-M. Wu, and S.-F. Tsay, J. Chem. Phys. **132**, 034502 (2010).
[30]T. Scopigno, A. Filipponi, M. Krisch, G. Monaco, G. Ruocco, and F. Sette, Phys. Rev. Lett. **89**, 255506 (2002).
[31]T. Scopigno, R. Di Leonardo, L. Comez, A. Q. R. Baron, D. Fioretto, and G. Ruocco, Phys. Rev. Lett. **94**, 155301 (2005).
[32]S. Hosokawa, W.-C. Pilgrim, H. Sinn, and E. E. Alp, J. Phys.: Condens. Matter **20**, 114107 (2008).
[33]F. J. Bermejo, I. Bustinduy, S. J. Levett, J. W. Taylor, R. Fernández-Perea, and C. Cabrillo, Phys. Rev. B **72**, 104103 (2005).
[34]J. Yang, J. S. Tse, and T. Iitaka, J. Chem. Phys. **135**, 044507 (2011).
[35]L. E. González, D. J. González, and M. J. Stott, Phys. Rev. B **77**, 014207 (2008).
[36]Y. Katayama and K. Tsuji, J. Phys.: Condens. Matter **15**, 6085 (2003).
[37]W. Utsumi, K. Funakoshi, Y. Katayama, M. Yamakata, T. Okada, and O. Shimomura, J. Phys.: Condens. Matter **14**, 10497 (2002).
[38]D. L. Decker, J. Appl. Phys. **42**, 3239 (1971).
[39]K. Tsuji, K. Yaoita, M. Imai, O. Shimomura, and T. Kikegawa, Rev. Sci. Instrum. **60**, 2425 (1989).
[40]K. Funakoshi, Ph.D. thesis, Tokyo Institute of Technology, 1997.
[41]R. Kaplow, S. L. Strong, and B. L. Averbach, Phys. Rev. **138**, A1336 (1965).
[42]W. H. Press, S. A. Teukolsky, W. T. Vetterling, and B. P. Flannery, *Numerical Recipes in C: The Art of Scientific Computing*, 2nd ed. (Cambridge University Press, New York, 1992).
[43]H. Köster, F. Hensel, and E. U. Franck, Ber. Bunsen-Ges. Phys. Chem. **74**, 43 (1970).
[44]O. Gereben, P. Jovari, L. Temleitner, and L. Pusztai, J. Optoelectron.: Adv. Mater. **9**, 3021 (2007).
[45]L. Bosio, J. Chem. Phys. **68**, 1221 (1978).
[46]A. Jayaraman, W. Klement Jr., R. Newton, and G. Kennedy, J. Phys. Chem. Solids **24**, 7 (1963).
[47]Y. Waseda, *The Structure of Non-Crystalline Materials: Liquids and Amorphous Solids* (McGraw-Hill, New York, 1980).
[48]Y. Morimoto, S. Kato, N. Toda, Y. Katayama, K. Tsuji, K. Yaoita, and O. Shimomura, Rev. High Press. Sci. Technol. **7**, 245 (1998).
[49]K. Tsuji, *Elementary Processes in Dense Plasmas: The Proceedings of the Oji International Seminar (Frontiers in Physics)*, edited by S. Ichimaru and S. Ogata (Addison-Wesley, New York, 1980).
[50]N. S. Gingrich and C. W. Tompson, J. Chem. Phys. **36**, 2398 (1962).
[51]R. L. McGreevy, A. Baranyai, and I. Ruff, Phys. Chem. Liq. **16**, 47 (1986).
[52]M. A. Howe, R. L. McGreevy, L. Pusztai, and I. Borzsak, Phys. Chem. Liq. **25**, 205 (1993).

[53]J. Z. Jiang, W. Roseker, M. Sikorski, Q. P. Cao, and F. Xu, Appl. Phys. Lett. **84**, 1871 (2004).
[54]Q.-s. Zeng, Y. Ding, W. L. Mao, W. Yang, S. V. Sinogeikin, J. Shu, H.-k. Mao, and J. Z. Jiang, Phys. Rev. Lett. **104**, 105702 (2010).
[55]D. Ma, A. D. Stoica, and X.-L. Wang, Nat. Mater. **8**, 30 (2009).
[56]C. Meade, R. J. Hemley, and H. K. Mao, Phys. Rev. Lett. **69**, 1387 (1992).
[57]T. Hattori, K. Tsuji, N. Taga, Y. Takasugi, and T. Mori, Phys. Rev. B **68**, 224106 (2003).
[58]H. Schafer, Ber. Bunsen-Ges. Phys. Chem. **79**, 110 (1975).
[59]K. Takemura, K. Kobayashi, and M. Arai, Phys. Rev. B **58**, 2482 (1998).